JACS
JOURNAL OF THE AMERICAN CHEMICAL SOCIETY
Article
pubs.acs.org/JACS

Chiral Sum Frequency Generation for In Situ Probing Proton Exchange in Antiparallel β-Sheets at Interfaces

Li Fu,[†] Dequan Xiao,[†] Zhuguang Wang, Victor S. Batista,* and Elsa C. Y. Yan*

Department of Chemistry, Yale University, 225 Prospect Street, New Haven, Connecticut 06520, United States

Supporting Information

ABSTRACT: Studying hydrogen/deuterium (H/D) exchange in proteins can provide valuable insight on protein structure and dynamics. Several techniques are available for probing H/D exchange in the bulk solution, including NMR, mass spectroscopy, and Fourier transform infrared spectroscopy. However, probing H/D exchange at interfaces is challenging because it requires surface-selective methods. Here, we introduce the combination of in situ chiral sum frequency generation (cSFG) spectroscopy and ab initio simulations of cSFG spectra as a powerful methodology to probe the dynamics of H/D exchange at interfaces. This method is applied to characterize H/D exchange in the antiparallel β-sheet peptide LK$_7\beta$. We report here for the first time that the rate of D-to-H exchange is about 1 order of magnitude faster than H-to-D exchange in the antiparallel structure at the air/water interface, which is consistent with the existing knowledge that O−H/D dissociation in water is the rate-limiting step, and breaking the O−D bond is slower than breaking the O−H bond. The reported analysis also provides fundamental understanding of several vibrational modes and their couplings in peptide backbones that have been difficult to characterize by conventional methods, including Fermi resonances of various combinations of peptide vibrational modes such as amide I and amide II, C−N stretch, and N−H/N−D bending. These results demonstrate cSFG as a sensitive technique for probing the kinetics of H/D exchange in proteins at interfaces, with high signal-to-noise N−H/N−D stretch bands that are free of background from the water O−H/O−D stretch.

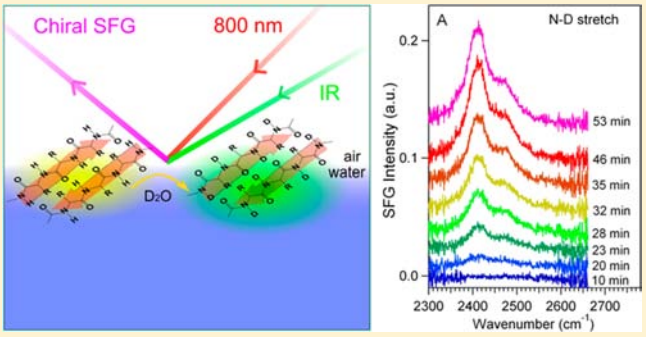

INTRODUCTION

Probing hydrogen/deuterium (H/D) exchange in proteins in bulk solutions has proven very useful to reveal protein dynamics and structures.[1] NMR,[2] mass spectrometry (MS),[3] and Fourier transform infrared spectroscopy (FTIR)[4] have been used to probe H/D exchange in protein to yield information about structures of intermediates of protein folding,[5,6] kinetics and structures of amyloid aggregation,[7−11] and conformational changes of proteins upon ligand binding.[12−14] Nonetheless, there is a lack of surface-selective methods that allow real-time and in situ characterization of H/D exchange in proteins at interfaces. Such characterization is expected to be useful to reveal interactions among proteins, water, and biomembranes, enabling investigations, such as solvent accessibility of proteins embedded in membranes, proton transfer,[15] and intramolecular hydrogen-bonding interactions[16] in membrane proteins, and water channels formed by transmembrane proteins.[17,18]

Although the peptide N−H/N−D stretch can directly reveal proton exchange in proteins, characterization of the N−H/N−D stretch of proteins in aqueous environments using conventional vibrational methods has remained challenging. The challenge comes from the overwhelming O−H/O−D stretch of water background that overlaps with the N−H/N−D stretch. We recently demonstrated that chiral sum frequency generation (cSFG) spectroscopy can probe peptide N−H stretch with zero water background.[19] On the basis of this finding, we introduce cSFG as a method for in situ probing H/D exchange in proteins at interfaces in real time.

Both experimental approaches[19−24] and theory[25−30] of sum frequency generation spectroscopy have been evolving in a fast pace. These developments have served as a basis to establish cSFG as a biophysical analytical tool to characterize biointerfaces.[31] It has been applied to study various biomolecules, including DNA[32,33] and proteins.[19,24,31] Recently, we found that cSFG can provide a set of vibrational optical signatures for characterizing protein secondary structures at interfaces,[19,31] similar to the use of circular dichroism (CD) spectroscopy to characterize protein secondary structures in bulk solution. The N−H stretch along the peptide backbones at ~3300 cm^{-1} probed by cSFG is characteristic of β-sheet and α-helical structures at interfaces.[31] Using this chiral N−H stretch together with the chiral amide I signal, we studied the misfolding of human islet amyloid polypeptide (hIAPP), an amyloid protein associated with type II diabetes, upon interactions with a lipid/water interface. We observed the

Received: December 7, 2012
Published: February 8, 2013

   dx.doi.org/10.1021/ja3119527 | J. Am. Chem. Soc. 2013, 135, 3592−3598

misfolding of hIAPP from disordered structures to α-helical structures and then to β-sheet structures in situ and in real time.

In this study, we used the LK$_7\beta$ peptide, which has a sequence of LKLKLKL.[34] This peptide forms an antiparallel β-sheet at amphiphilic interfaces. It has been extensively characterized by a wide range of methods, including CD,[34] FTIR,[34] and conventional (achiral) SFG.[35−37] Chen and co-workers probed antiparallel β-sheets using cSFG, focusing on the amide I vibrational modes. They observed a strong amide I signal.[24] In general, antiparallel β-sheets adopt D_2 symmetry, which is proposed to give strong nonlinear optical response.[38,39] Indeed, when we used cSFG to characterize the structure of LK$_7\beta$ at the air/water interface in this study, we observed that LK$_7\beta$ at the air/water interface exhibits strong cSFG signals of peptide backbone in both N−H/N−D stretch and amide I regions. Using the N−H/N−D stretch signals, we monitor the H/D exchange of LK$_7\beta$ at the air/water interface upon H_2O/D_2O solvent exchange in situ and in real time.

Our cSFG spectra of LK$_7\beta$ in the N−H and N−D stretch regions exhibit subtle vibrational features, which have not been observed by conventional vibrational spectroscopies due to the overwhelming O−H/O−D stretch water background. To analyze these spectral features, we performed ab initio SFG simulation and normal-mode analysis to explore various possibilities of assigning these vibrational features, which include amide I/amide II combinational band, amide I and amide II overtones, free N−H group exposed to the solvent environment, and C−N stretch/N−D bending combinational band. Understanding these vibrational features can reveal coupling of various vibrational modes along peptide backbones, which is fundamentally important for investigations of vibrational energy redistribution in proteins in aqueous environments.

EXPERIMENTAL SECTION

cSFG Experiments. We obtained the cSFG spectra of LK$_7\beta$ peptide at the air/water interface using our broadband SFG spectrometer,[40] which is described in Ma et al. and the Supporting Information. In this study, the *psp* polarization setting (*p*-polarized SFG, *s*-polarized visible, and *p*-polarized IR) was used for cSFG detection. We first obtained the chiral amide I spectra, and then N−H and N−D spectra using H_2O and D_2O as the solvent, respectively. To probe the H-to-D exchange, we added D_2O into the H_2O solution of LK$_7\beta$ to initiate the exchange process and then monitored the N−D stretch spectra. In the experiments, we used a final ratio of D_2O:H_2O equal to 1:4 (1.00 mL of D_2O into 4.00 mL of H_2O) or 1:2 (1.67 mL of D_2O into 3.33 mL of H_2O). Similarly, to probe the D-to-H exchange, we added H_2O into the D_2O solution of LK$_7\beta$ and then monitored the N−H stretch spectra. D_2O or H_2O was added along the side of the Teflon beaker without additional stirring to avoid surface perturbation.

Materials and Data Acquisition. The LK$_7\beta$ peptide was synthesized and purified by the W.M. Keck Biotechnology Resource Laboratory at Yale University. The lyophilized LK$_7\beta$ peptide was dissolved in deionized water and distributed into vials, which were frozen in liquid nitrogen and stored at −80 °C. Each vial of the solution was thawed for one SFG experiment and never frozen again. In the SFG experiments, a Teflon beaker containing phosphate buffer (10 mM phosphate, pH/pD = 7.4) was placed on the sample stage. The pD values were obtained using a correction of pD = pH + 0.4.[41,42] A stock solution of LK$_7\beta$ was added using a microsyringe to give a final concentration of 25 μM. The H/D exchange was initiated by adding D_2O into H_2O, or adding H_2O into D_2O. While each cSFG spectrum in the kinetic studies was taken with an acquisition time of 1 min, other spectra were taken with an acquisition time of 10 min. The raw spectra were processed by the steps of removing the contribution from cosmic rays, subtracting background, calibrating the wavenumber, and normalizing to the IR power, as previously desecribed.[40] The processed spectra were then fitted into the following equation:

$$I_{SFG} \propto \left| \chi_{NR}^{(2)} + \sum_q \frac{A_q}{\omega_{IR} - \omega_q + i\Gamma} \right|^2 \quad (1)$$

where I_{SFG} is the sum frequency generation intensity, χ_{NR} is the nonresonant second-order susceptibility, ω_{IR} is the input IR frequency, and A_q, ω_q, and Γ_q are the amplitude, resonant frequency, and damping factor of the qth vibration mode, respectively.

Ab Initio Simulation of SFG Spectra. We built an antiparallel β-sheet model using two peptides. Each contains four glycine residues and two cysteine residues. The two peptides are linked to each other in an antiparallel configuration by two disulfide bonds at the ends of the peptides (Scheme 1), forming an antiparallel β-sheet. The Gaussian 09 program[43] was used to perform geometry optimization and normal-mode analysis at the density functional theory (DFT) level for the antiparallel β-sheet, using the B3LYP functional and the 6-31G* basis set. With the same DFT method and basis set, the dipole derivatives $\partial\mu_n/\partial Q_q$ and polarizability derivatives $\partial\alpha_{lm}/\partial Q_q$ (where n, l, m are the indexes of directions in the Cartesian coordinate, and Q denotes for the normal mode coordinate) for the qth normal mode were computed using the keywords "iop(7/33=1)" and "polar", respectively. The computed $\partial\mu_n/\partial Q_q$ and $\partial\alpha_{lm}/\partial Q_q$ yield the vibrational hyperpolarizability tensors through $\beta_{lmn,q} \propto ((\partial\alpha_{lm})/(\partial Q_q))\cdot((\partial\mu_n)/(\partial Q_q))$. Finally, we computed the second-order susceptibility tensor elements using Euler transformation, and simulated the *psp* cSFG spectra as described in our previous work.[44] To compare the calculated SFG spectra with the experiment spectra, the calculated vibrational frequencies of all of the normal modes in this study were scaled using a common factor of 0.9322.

Scheme 1. An Antiparallel β-Sheet Model Consisting of Glycine Repeat Units and Two Disulfide Bonds Formed by Cysteine Residues Used for cSFG Simulations

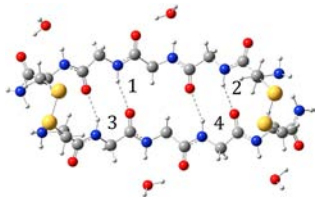

RESULTS

In this section, we will first present the cSFG spectra of LK$_7\beta$ at the air/water interface in the amide I region, and then the N−H and N−D stretch regions using H_2O and D_2O as solvent, respectively. Subsequently, we will show how cSFG can be used to monitor the kinetics of H/D exchange in LK$_7\beta$ at the air/water interface using the chiral N−D and N−H stretch vibrational modes. Finally, we report the results of ab initio calculations and peak assignments in the N−H and N−D stretch spectra of LK$_7\beta$.

Amide I Spectra at the Air/Water Interfaces. We obtained the cSFG spectrum of LK$_7\beta$ at the air/H_2O interface in the amide I region. The spectrum shows a peak at 1619 cm^{-1} and a shoulder at 1690 cm^{-1} (Figure 1), which are the characteristic B_2 mode and B_1 mode of the amide I vibrations of antiparallel β-sheets, respectively.[24] These peak positions agree with previous characterizations using FTIR and polarized modulated infrared reflection-adsorption spectroscopy (IRRAS) methods.[45,46] We also obtained the chiral amide I spectrum of LK$_7\beta$ at the air/D_2O interface and observed that

dx.doi.org/10.1021/ja3119527 | J. Am. Chem. Soc. 2013, 135, 3592−3598

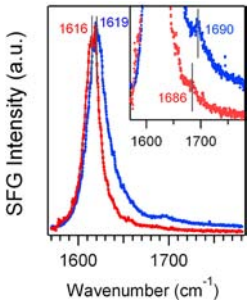

Figure 1. Chiral amide I spectra of LK$_7\beta$ at the air/H_2O interface (blue) and air/D_2O interface (red).

the B_2 band shifts from 1619 to 1616 cm^{-1} (Figure 1). This kind of red shift in the amide I band is commonly observed in various protein secondary structures due to the isotope shift of the N−H/N−D in-plane bending mode that contributes to the amide I band.[47,48] The B_1 band in the D_2O spectrum becomes less obvious (Figure 1, inset). The observation of the characteristic B_2 mode (1620 cm^{-1}) and B_1 mode (1690 cm^{-1}) of the amide I vibrations at the air/H_2O interface indicates that LK$_7\beta$ forms antiparallel β-sheet structures.

N−H/N−D Stretch Spectra at the Air/Water Interfaces. We obtained the N−H and N−D stretch spectra of LK$_7\beta$ at the air/H_2O and air/D_2O interfaces, respectively (Figure 2). These

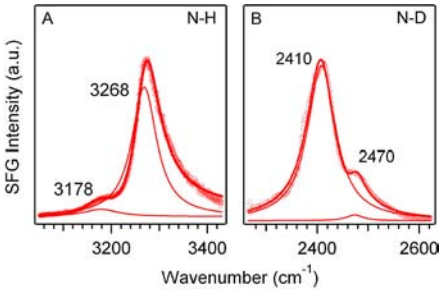

Figure 2. Chiral SFG spectra of LK$_7\beta$ (A) in the N−H stretch region at the air/H_2O interface and (B) in the N−D stretch region at the air/D_2O interface.

spectra were fitted into eq 1, and the fitting parameters are summarized in Table 1. The fitting results show that the N−H

Table 1. Spectral Parameters Obtained by Fitting the Chiral N−H and N−D Spectra (Figure 2) into Equation 1

spectra	fitting parameters	values
N−H stretch (Figure 2A)	χ_{NR} (au)	0.154 ± 0.002
	ω_1 (cm^{-1})	3178 ± 0.8
	A_1 (au)	9.6 ± 0.4
	Γ_1 (au)	43.6 ± 1.8
	ω_2 (cm^{-1})	3268 ± 0.1
	A_2 (au)	29.2 ± 0.3
	Γ_2 (au)	31.6 ± 0.2
N−D stretch (Figure 2B)	χ_{NR} (au)	−0.008 ± 0.002
	ω_1 (cm^{-1})	2473 ± 0.4
	A_1 (au)	2.6 ± 0.2
	Γ_1 (au)	20.2 ± 1.0
	ω_2 (cm^{-1})	2409 ± 0.2
	A_2 (au)	21.9 ± 0.1
	Γ_2 (au)	33.4 ± 0.2

spectrum exhibits a peak at 3268 cm^{-1} and a shoulder at 3178 cm^{-1}, while the N−D spectrum displays a peak at ∼2410 cm^{-1} and a shoulder at ∼2470 cm^{-1}. We will discuss the assignments of these vibrational bands in the spectral analysis section.

H/D Exchange of LK$_7\beta$ at the Air/Water Interface. We used the chiral N−D and N−H stretch signals (Figure 2) to monitor the kinetics of proton exchange in LK$_7\beta$ at interfaces. We initiated the H/D exchange process upon addition of D_2O into the H_2O solution of LK$_7\beta$ or addition of H_2O into the D_2O solution of LK$_7\beta$. Figure 3 shows the time-dependent

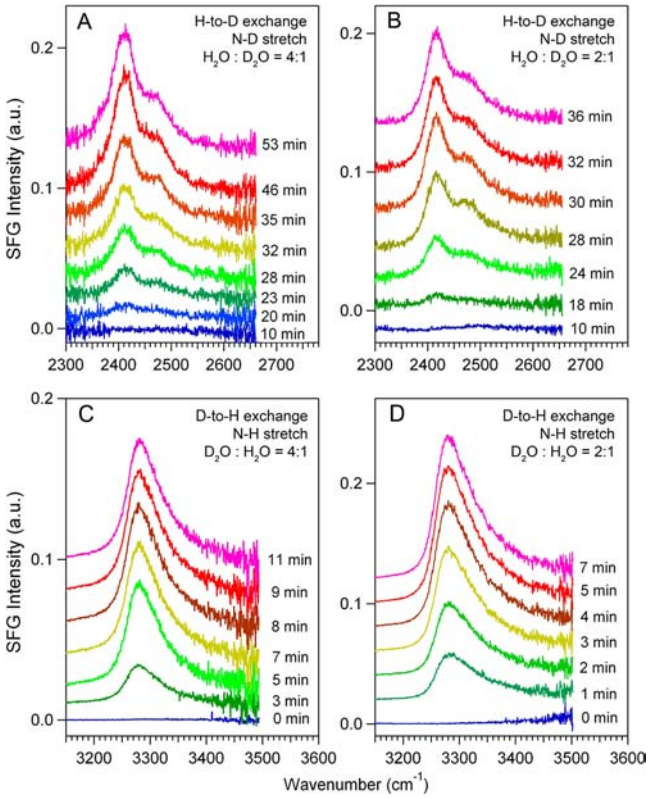

Figure 3. Kinetics of H/D exchange in LK$_7\beta$ at the air/water interface. Time-dependent N−D stretch spectra of LK$_7\beta$ at the air/H_2O interface upon addition of D_2O at a ratio of H_2O:D_2O equal to (A) 4:1 and (B) 2:1. Time-dependent N−H stretch spectra of LK$_7\beta$ at the air/D_2O interface upon addition of H_2O at a ratio of D_2O:H_2O equal to (C) 4:1 and (D) 2:1.

cSFG spectra of LK$_7\beta$ in the N−D and N−H stretch regions. Figure 3A and B presents the kinetics of H-to-D exchange (addition of D_2O to H_2O) with a final H_2O:D_2O ratio of 4:1 and 2:1, respectively. The N−D signals gradually build up in the spectra. Similarly, Figure 3C and D presents the kinetics of D-to-H exchange (addition of H_2O to D_2O) with a final H_2O:D_2O ratio of 1:4 and 1:2, respectively. The N−H signals gradually increase upon addition of H_2O. These results demonstrate the in situ and real-time kinetics of the proton exchange along the peptide backbone of LK$_7\beta$ at the air/water interface.

Figure 3 shows that the rates of H-to-D and D-to-H exchange are different. For the systems with a ratio of 4:1 (D_2O:H_2O or H_2O:D_2O), the H-to-D exchange (Figure 3A) takes ∼50 min to complete, while the D-to-H exchange (Figure 3C) takes ∼10 min. Similarly, for the systems with a ratio of 2:1 (D_2O:H_2O or H_2O:D_2O), the H-to-D exchange (Figure 3B)

dx.doi.org/10.1021/ja3119527 | J. Am. Chem. Soc. 2013, 135, 3592−3598

takes ~30 min, while the D-to-H exchange (Figure 3D) takes ~5 min. Figure 4 shows the plots of SFG field for the N−H

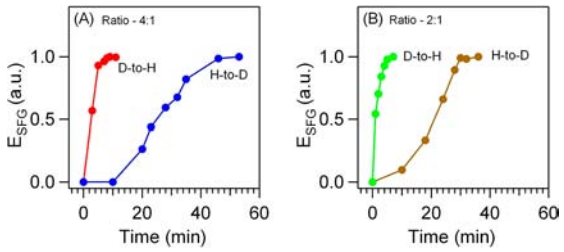

Figure 4. The time dependence of the SFG field: (A) D-to-H exchange with H_2O:D_2O 4:1 (red) and H-to-D exchange with D_2O:H_2O 4:1 (blue), and (B) D-to-H exchange with D_2O:H_2O 2:1 (green) and H-to-D exchange with H_2O:D_2O 2:1 (brown).

(3268 cm^{-1}) and N−D (2410 cm^{-1}) stretch as a function of time. The plots can be fitted into a stretched exponential function (Supporting Information), which reveal the empirical relaxation of the D-to-H exchange in 1 order of magnitude faster than that of the H-to-D exchange. We realize that this empirical comparison is qualitative; however, a quantitative comparison requires a development and validation of a kinetic model, which is out of the scope of our current study that is to develop cSFG as a new method for probing real-time kinetics of proton exchange in proteins at aqueous interfaces.

Spectral Analyses and Ab Initio SFG Simulations. We performed ab initio SFG simulation and normal-mode analysis to reveal the origin of experimentally observed chiral N−H and N−D stretch vibrational bands in Figure 2, where the N−H spectrum (Figure 2A) shows a major peak at 3268 cm^{-1} and a shoulder at 3178 cm^{-1}, while the N−D spectrum (Figure 2B) shows a major peak at 2410 cm^{-1} and a shoulder at 2470 cm^{-1}.

We started by assigning the major peaks in the cSFG spectra of LK$_7\beta$ (Figure 2). We ascribe the major peaks at 3268 cm^{-1} (Figure 2A) and 2410 cm^{-1} (Figure 2B) to the N−H and N−D stretches of the peptide backbone, respectively. These assignments are consistent with Rozenberg and Shoham's assignment for nondeuterated and deuterated antiparallel β-sheets.[49] They used FTIR to study antiparallel β-sheets formed by poly lysines and found that the N−H stretch frequency is at 3270 cm^{-1}, while the N−D stretch frequency is shifted to 2410 cm^{-1}. Moreover, we performed ab initio calculations to simulate the cSFG spectra (Figure 5). The normal-mode analysis suggests

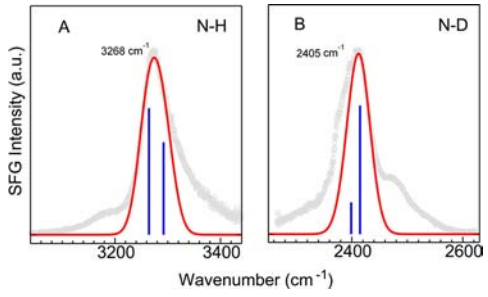

Figure 5. Calculated *psp* cSFG spectra (i.e., red curves) of nondeuterated and deuterated LK$_7\beta$: (A) N−H stretch region and (B) N−D stretch region, where the gray circles are the experimental spectra, and the blue sticks denote the effective *psp* 2nd susceptibilities squared[44] contributed by individual normal modes. The scaling factor is 0.9322 for the calculated spectra.

that N−H and N−D stretches of the antiparallel β-sheets are both IR and Raman active, rendering SFG activity. Using a common scaling factor of 0.9322, the major peak in the N−H spectrum appears at 3268 cm^{-1} (Figure 5A), while the major peak in the N−D spectrum appears at 2405 cm^{-1} (Figure 5B). This relative positioning of major peaks between the N−H and N−D stretches agree with our experimental results (Figure 2).

Besides the major peaks, the cSFG spectra also show shoulder peaks at ~3178 cm^{-1} in the N−H spectrum (Figure 2A) and ~2470 cm^{-1} in the N−D spectrum (Figure 2B). Becauase these spectral features have never been reported previously, we assigned these peaks based on the normal-mode analysis from ab initio calculations and additional chiral SFG experiments. We explored the following possibilities for the assignments: (i) amide II overtone, (ii) amide I overtone, and (iii) N−H stretch of free N−H groups (i.e., the N−H groups exposed to the solvent). However, the results of our calculations and additional control experiments prompt us to eliminate these possibilities based on unmatched calculated frequencies, which are discussed in the Supporting Information. Subsequently, we tentatively assign the 3178 cm^{-1} shoulder peak to the Fermi resonance of the combinational band of the amide I and amide II modes with the N−H stretch, and the 2470 cm^{-1} shoulder peak to the Fermi resonance of the combination band of the C−N stretch and the N−D in-plane bending with the N−D stretch (Table 2). Below, we elucidate the rationale for these assignments.

Table 2. Experimental Observed and Calculated Vibrational Frequencies

peak assignment		exp. (cm^{-1})		calc. (cm^{-1})	
N−H stretch		3268		3268	
amide I	combination	1619	3178	1626	3171
amide II		1563		1545	
N−D stretch		2410		2416	
C−N stretch	combination	1470	2473	1422	2466
N−D bending		N/A		1044	

First, we discuss the 3178 cm^{-1} shoulder peak in the N−H spectrum (Figure 2A). According to previous studies, the ~3178 cm^{-1} peak can possibly be due to the Fermi resonance of the combinational mode of amide I and amide II.[50] To test this possibility, we performed normal-mode analyses in the N−H stretch regions of the antiparallel β-sheet model (Scheme 1). The computed vibrational frequency is 1626 cm^{-1} for amide I and 1545 cm^{-1} for amide II. The combination band should have a frequency of ~3171 cm^{-1}, which is close to the experimental value (3178 cm^{-1}). To confirm this assignment, we further obtained the amide II spectrum of LK$_7\beta$ (Figure S1), which shows an amide II band at 1563 cm^{-1}. Because the amide I band is at 1619 cm^{-1} (Figure 1), the combination band of amide I and amide II is at 3182 cm^{-1}, which is close to 3178 cm^{-1}. Hence, we attribute the shoulder peak at 3178 cm^{-1} (Figure 2A) to the Fermi resonance of a combination band due to amide I and amide II with N−H stretch.

We then discuss the assignment of the 2473 cm^{-1} shoulder peak (Figure 2B). The peak can possibly be due to the Fermi resonance of a combinational band of C−N stretch and N−D in-plane bending with the N−D stretch, as suggested by Krimm and co-workers.[51,52] We performed ab initio calculations to examine this assignment. Our calculation shows that the C−N stretch is at 1422 cm^{-1} and the N−D in-plane bending is at

dx.doi.org/10.1021/ja3119527 | J. Am. Chem. Soc. 2013, 135, 3592−3598

1044 cm^{-1}. Hence, the combination band is at 2466 cm^{-1}, which is close to the experimental value of 2473 cm^{-1}. To further test this assignment, we obtained the cSFG spectra of $LK_7\beta$ in the C−N stretch region (Figure S1) and observed a vibrational band at ∼1470 cm^{-1}. This frequency is deviated from the calculated value (1422 cm^{-1}). The red-shift of the calculated C−N stretch (amide II′) frequency could be attributed to the lack of explicit solvent interactions between amide groups and water as discussed in the literature.[53] We also attempted to experimentally obtain cSFG spectrum of $LK_7\beta$ in the N−D bending region (∼1000 cm^{-1}). Nonetheless, we were not able to observe the N−D bending band, which is perhaps due to our experimental limit of the lower IR energy in the 1000-cm^{-1} region, and/or the weak chiral SFG signal of the N−D bending mode as shown by the ab initio SFG simulations (Supporting Information). We also explored other possibilities of assigning the 2473 cm^{-1} peak, including the overtone of amide II′. Nonetheless, we eliminated these possibilities due to the poor agreement between the calculated and experimental frequencies (see the Supporting Information). Therefore, we ascribed the appearance of the 2473 cm^{-1} shoulder peak to the Fermi resonance of the combination band of C−N stretch and N−D in-plane bending with the N−D stretch.

DISCUSSION

Summary. We have used cSFG to monitor the N−H/N−D signals of the peptide backbone upon H_2O/D_2O solvent exchange and observed an in situ H/D exchange in $LK_7\beta$ at the air/water interface. We found that the rate of D-to-H exchange is faster than that of H-to-D exchange. Because cSFG is free of the background of water O−H stretches, we have observed subtle vibrational features that were difficult to observe using conventional vibrational methods. We found both the N−H and the N−D spectra show a major peak and a shoulder. The N−H spectrum exhibits a major peak at 3268 cm^{-1} and a red-shifted shoulder peak at 3178 cm^{-1}, while the N−D spectrum displays a major peak at 2410 cm^{-1} and a blue-shifted shoulder at 2473 cm^{-1}. We performed ab initio normal-mode analysis and assigned the shoulder peaks to the Fermi resonance between the N−H stretch and the combination band of amide I and amide II, and the Fermi resonance between the N−D stretch and the combination band of C−N stretch and N−D in-plane bending, respectively.

Differences in the Rates of D-to-H and H-to-D Exchange. We observed that the rates of D-to-H exchange are faster than the rates of H-to-D exchange by roughly 1 order of magnitude. This result suggests that the rate-determining step of the H/D exchange in $LK_7\beta$ at the air/water interface involves breaking the water O−H/O−D bond rather than the N−H/N−D bond of the peptide. Because the zero-point energy of the O−D stretch is lower than that of the O−H stretch, it needs higher energy to break an O−D bond than an O−H bond. For the H-to-D exchange in peptide, the rate-determining step is to break the O−D bond in water; thus, the activation energy is higher and the rate is slower. For the D-to-H exchange in peptide, the rate-determining step is to break the O−H bond in water. Hence, the activation energy is lower and the rate is faster. Ribeiro-Claro et al. used Raman spectroscopy to monitor the O−H/O−D stretch of crystalline α-cyclodextrin upon exposure to the H_2O/D_2O vapor. They found that the D-to-H exchange is 7−10 times faster than the H-to-D exchange and concluded that the rate-determining step of the H/D exchange is to break the O−H/O−D bond in water vapor,[54] which aligns with our interpretation. Moreover, Englander and co-workers also measured the H-to-D and D-to-H exchange using NMR for bulk solutions.[42] According to their results, the D-to-H exchange rate constant is about ∼5 times faster than that of H-to-D exchange at pH 6, which is also in agreement with our observations of proton exchange at interfaces.

Increases versus Decreases in the N−D/N−H Stretch Signals. In our experiments, we chose to monitor the increase of the N−D/N−H stretch signals rather than the decrease of the N−D/N−H stretch signals to study the kinetics of proton exchange in $LK_7\beta$ (Figure 2). When we examined the decrease in the N−H (N−D) signals in the H-to-D (D-to-H) exchange process, we indeed observed a substantial decrease of the N−H (N−D) signal toward the end of the exchange process (Figure S3 in the Supporting Information). However, at the beginning of the exchange, we observed fluctuations of the cSFG signal (Figure S4), which could be due to perturbation to the interface upon addition of H_2O/D_2O, and/or nonhomogeneous solution during the acquisition time. Nonetheless, when we monitored the increase of the N−H (N−D) signal in the D-to-H (H-to-D) exchange process, we detected the N−H (N−D) signal accumulating on top of zero background, which allows an observation of a steady increase of the N−H stretch signals that can reveal the kinetics of the exchange process.

N−H Stretch in the Lysine Side Chain. Although it is possible to assign the N−H/D−H stretch to the amine group of the lysine residue in $LK_7\beta$,[55] this assignment does not apply to our observed chiral N−H/N−D stretch signals under our experimental conditions, which is based on three considerations. First, the H/D exchange in charged side chains is known to be instantaneous or diffusion limited,[1] while the H/D exchange on the amide backbone has been previously shown to be on the time scale ranging from minutes to days.[1] Because we observed the exchange rates are on the time scale of minutes in our studies, the chiral N−H signal is not likely due to the lysine residue. Second, the $-NH_3^+$ group has the asymmetric N−H stretch at 3000−3200 cm^{-1} and the symmetric N−H stretch at 2100−2600 cm^{-1}. The cSFG spectrum (Figure 2) shows the chiral N−H stretch at 3300 cm^{-1}, which does not match with the N−H stretch frequencies of the $-NH_3^+$ group. Moreover, the phosphate buffer in our experiments maintained the bulk pH at 7.4, and the $-NH_3^+$ group of lysine has a pK_a at 10.5. Although the surface pK_a of lysine may change, a previous study performed by the Eisenthal group shows that the pK_a of $CH_3(CH_2)_{21}NH_3^+$ only changes from 10.7 to 9.9 at the air/water interface.[56] Thus, the lysine side chain should remain protonated at the air/water interface. Third, we previously showed that the α-helical $LK_{14}\alpha$ $(LKKLLKL)_2$ also exhibits chiral N−H signals. Because both $LK_{14}\alpha$ and $LK_7\beta$ contain only the lysine and leucine residues, if our observed chiral N−H stretch is due to the Lys residue, we would expect the N−H stretch frequency of the $LK_{14}\alpha$ and $LK_7\beta$ peptides to be the same. Nonetheless, the chiral N−H stretch of $LK_{14}\alpha$ is at 3304 cm^{-1},[19,31] while that of $LK_7\beta$ is at 3268 cm^{-1}. We previously attributed this 40 cm^{-1} shift in the chiral N−H stretch frequency to the different hydrogen-bonding environments of the peptide N−H group in different protein secondary structures. On the basis of these considerations, we assign the observed cSFG signals to the peptide backbone N−H stretch.

Sensitivity of cSFG in Detecting N−H/N−D Stretch in Aqueous Environments. Our results demonstrate that cSFG has the selectivity of chirality and interface to probe the N−H/N−D stretch of peptides free of the O−H stretch background

dx.doi.org/10.1021/ja3119527 | J. Am. Chem. Soc. 2013, 135, 3592−3598

of water. Because water molecules do not form chiral structures at interfaces, cSFG is muted to water O−H stretch signals. Thus, cSFG can provide N−H/N−D stretch spectra of proteins at interfaces in a high signal-to-noise level free of water background. Consequently, cSFG can be used to study detailed coupling of various vibrational modes of the peptide backbones in the N−H/N−D regions. These vibrational modes include the amide I, amide II, C−N stretch, and their various overtones and combinational modes. Except in the gas phase,[57,58] the studies of vibrational coupling in the N−H/N−D region in aqueous solution have been difficult using conventional vibrational methods because of the overwhelming broad O−H/O−D stretch band of water. Here, our results show that cSFG can tackle this problem, introducing a method for probing vibrational couplings and vibrational energy distribution along peptide backbones.

CONCLUSION

On the basis of our results, we conclude that cSFG spectroscopy is a label-free, background-free method to study real-time kinetics of proton exchange in proteins in situ at interfaces. Using cSFG to monitor the N−H/N−D stretch of the $LK_7\beta$ peptide backbone, we observed that the rate of D-to-H exchange is about an order of magnitude faster than that of H-to-D exchange in the $LK_7\beta$ antiparallel structure at the air/water interface. These results demonstrate that further applications of cSFG in characterizing the peptide N−H/N−D stretch can potentially address a number of important problems related to interactions of proteins with water and membrane. Because protein secondary structures are constructed by the peptide N−H/N−D hydrogen-bonding interactions, the hydrogen-bonding environments for the peptide N−H/N−D groups are different in different secondary structures. Because cSFG can be used to detect the N−H/N−D stretch frequencies in aqueous environments, cSFG can provide a new tool for characterizing protein secondary structures at interfaces. Moreover, being an optical method, cSFG can be used to characterize the N−H/N−D peptide stretch in situ and in real time. Thus, it can provide kinetic information to reveal protein stability and protein folding at interface. We expect that further experimental developments of the cSFG method can allow investigations of solvent accessibility of proteins embedded in membranes, proton transfer across membrane mediated by proteins, and intermolecular and intramolecular hydrogen-bonding interactions in transmembrane proteins.

ASSOCIATED CONTENT

Supporting Information

Description of the materials and method, spectral analysis and ab initio calculation, and supplementary figures. This material is available free of charge via the Internet at http://pubs.acs.org.

AUTHOR INFORMATION

Corresponding Author

elsa.yan@yale.edu; victor.batista@yale.edu

Author Contributions

†These authors contributed equally.

Notes

The authors declare no competing financial interest.

ACKNOWLEDGMENTS

The authors thank Prof. Patrick Loria (Yale University) for helpful discussion. E.C.Y.Y. is the recipient of the Starter Grant Award, Spectroscopy Society of Pittsburgh. This work is supported by the National Science Foundation (NSF) Grant CHE 1213362. V.S.B. acknowledges supercomputer time from NERSC and support from the National Science Foundation (NSF) Grant CHE 0911520, and the National Institutes of Health (NIH) Grants 1R01 GM-084267-01 and GM-043278 for methods development.

REFERENCES

(1) Englander, S. W.; Downer, N. W.; Teitelba, H. *Annu. Rev. Biochem.* **1972**, *41*, 903−924.
(2) Wand, A. J.; Roder, H.; Englander, S. W. *Biochemistry* **1986**, *25*, 1107−1114.
(3) Engen, J. R. *Anal. Chem.* **2009**, *81*, 7870−7875.
(4) Zhang, Y. P.; Lewis, R. N. A. H.; Hodges, R. S.; McElhaney, R. N. *Biochemistry* **1992**, *31*, 11572−11578.
(5) Englander, S. W. *Annu. Rev. Biophys. Biomol. Struct.* **2000**, *29*, 213−238.
(6) Baldwin, R. L. *Curr. Opin. Struct. Biol.* **1993**, *3*, 84−91.
(7) Tobler, S. A.; Fernandez, E. J. *Protein Sci.* **2002**, *11*, 1340−1352.
(8) Kheterpal, I.; Wetzel, R. *Acc. Chem. Res.* **2006**, *39*, 584−593.
(9) Qi, W.; Zhang, A.; Patel, D.; Lee, S.; Harrington, J. L.; Zhao, L.; Schaefer, D.; Good, T. A.; Fernandez, E. J. *Biotechnol. Bioeng.* **2008**, *100*, 1214−1227.
(10) Wilson, L. M.; Mok, Y.-F.; Binger, K. J.; Griffin, M. D. W.; Mertens, H. D. T.; Lin, F.; Wade, J. D.; Gooley, P. R.; Howlett, G. J. *J. Mol. Biol.* **2007**, *366*, 1639−1651.
(11) Lu, X.; Wintrode, P. L.; Surewicz, W. K. *Proc. Natl. Acad. Sci. U.S.A.* **2007**, *104*, 1510−1515.
(12) Busenlehner, L. S.; Armstrong, R. N. *Arch. Biochem. Biophys.* **2005**, *433*, 34−46.
(13) Paterson, Y.; Englander, S. W.; Roder, H. *Science* **1990**, *249*, 755−759.
(14) Powell, K. D.; Ghaemmaghami, S.; Wang, M. Z.; Ma, L. Y.; Oas, T. G.; Fitzgerald, M. C. *J. Am. Chem. Soc.* **2002**, *124*, 10256−10257.
(15) le Coutre, J.; Gerwert, K. *FEBS Lett.* **1996**, *398*, 333−336.
(16) Garczarek, F.; Gerwert, K. *Nature* **2006**, *439*, 109−112.
(17) Murata, K.; Mitsuoka, K.; Hirai, T.; Walz, T.; Agre, P.; Heymann, J. B.; Engel, A.; Fujiyoshi, Y. *Nature* **2000**, *407*, 599−605.
(18) Zhu, F. Q.; Tajkhorshid, E.; Schulten, K. *FEBS Lett.* **2001**, *504*, 212−218.
(19) Fu, L.; Liu, J.; Yan, E. C. Y. *J. Am. Chem. Soc.* **2011**, *133*, 8094−8097.
(20) Belkin, M. A.; Han, S. H.; Wei, X.; Shen, Y. R. *Phys. Rev. Lett.* **2001**, *87*, 113001−1−113001−4.
(21) Belkin, M. A.; Kulakov, T. A.; Ernst, K. H.; Yan, L.; Shen, Y. R. *Phys. Rev. Lett.* **2000**, *85*, 4474−4477.
(22) Fu, L.; Ma, G.; Yan, E. C. Y. *J. Am. Chem. Soc.* **2010**, *132*, 5405−5412.
(23) Ji, N.; Shen, Y. R. *Chirality* **2006**, *18*, 146−158.
(24) Wang, J.; Chen, X. Y.; Clarke, M. L.; Chen, Z. *Proc. Natl. Acad. Sci. U.S.A.* **2005**, *102*, 4978−4983.
(25) Haupert, L. M.; Simpson, G. J. *Annu. Rev. Phys. Chem.* **2009**, *60*, 345−365.
(26) Perry, J. M.; Moad, A. J.; Begue, N. J.; Wampler, R. D.; Simpson, G. J. *J. Phys. Chem. B* **2005**, *109*, 20009−20026.
(27) Simpson, G. J. *J. Chem. Phys.* **2002**, *117*, 3398−3410.
(28) Simpson, G. J. *ChemPhysChem* **2004**, *5*, 1301−1310.
(29) Auer, B. M.; Skinner, J. L. *J. Phys. Chem. B* **2008**, *113*, 4125−4130.
(30) Auer, B. M.; Skinner, J. L. *Chem. Phys. Lett.* **2009**, *470*, 13−20.
(31) Fu, L.; Wang, Z.; Yan, E. C. Y. *Int. J. Mol. Sci.* **2011**, *12*, 9404−9425.
(32) Walter, S. R.; Geiger, F. M. *J. Phys. Chem. Lett.* **2009**, *1*, 9−15.

(33) Stokes, G. Y.; Gibbs-Davis, J. M.; Boman, F. C.; Stepp, B. R.; Condie, A. G.; Nguyen, S. T.; Geiger, F. M. *J. Am. Chem. Soc.* **2007**, *129*, 7492−7493.
(34) DeGrado, W. F.; Lear, J. D. *J. Am. Chem. Soc.* **1985**, *107*, 7684−7689.
(35) Weidner, T.; Apte, J. S.; Gamble, L. J.; Castner, D. G. *Langmuir* **2009**, *26*, 3433−3440.
(36) Weidner, T.; Breen, N. F.; Li, K.; Drobny, G. P.; Castner, D. G. *Proc. Natl. Acad. Sci. U.S.A.* **2010**, *107*, 13288−13293.
(37) Mermut, O.; Phillips, D. C.; York, R. L.; McCrea, K. R.; Ward, R. S.; Somorjai, G. A. *J. Am. Chem. Soc.* **2006**, *128*, 3598−3607.
(38) Ostroverkhov, V.; Ostroverkhova, O.; Petschek, R. G.; Singer, K. D.; Sukhomlinova, L.; Twieg, R. J. *IEEE J. Sel. Top. Quantum Electron.* **2001**, *7*, 781−792.
(39) Ostroverkhov, V.; Singer, K. D.; Petschek, R. G. *J. Opt. Soc. Am. B* **2001**, *18*, 1858−1865.
(40) Ma, G.; Liu, J.; Fu, L.; Yan, E. C. Y. *Appl. Spectrosc.* **2009**, *63*, 528−537.
(41) Glasoe, P. K.; Long, F. A. *J. Phys. Chem.* **1960**, *64*, 188−190.
(42) Connelly, G. P.; Bai, Y. W.; Jeng, M. F.; Englander, S. W. *Proteins* **1993**, *17*, 87−92.
(43) Frisch, M. J.; Trucks, G. W.; Schlegel, H. B.; Scuseria, G. E.; Robb, M. A.; Cheeseman, J. R.; Montgomery, J. A., Jr.; Vreven, T.; Kudin, K. N.; Burant, J. C.; Millam, J. M.; Iyengar, S. S.; Tomasi, J.; Barone, V.; Mennucci, B.; Cossi, M.; Scalmani, G.; Rega, N.; Petersson, G. A.; Nakatsuji, H.; Hada, M.; Ehara, M.; Toyota, K.; Fukuda, R.; Hasegawa, J.; Ishida, M.; Nakajima, T.; Honda, Y.; Kitao, O.; Nakai, H.; Klene, M.; Li, X.; Knox, J. E.; Hratchian, H. P.; Cross, J. B.; Bakken, V.; Adamo, C.; Jaramillo, J.; Gomperts, R.; Stratmann, R. E.; Yazyev, O.; Austin, A. J.; Cammi, R.; Pomelli, C.; Ochterski, J. W.; Ayala, P. Y.; Morokuma, K.; Voth, G. A.; Salvador, P.; Dannenberg, J. J.; Zakrzewski, V. G.; Dapprich, S.; Daniels, A. D.; Strain, M. C.; Farkas, O.; Malick, D. K.; Rabuck, A. D.; Raghavachari, K.; Foresman, J. B.; Ortiz, J. V.; Cui, Q.; Baboul, A. G.; Clifford, S.; Cioslowski, J.; Stefanov, B. B.; Liu, G.; Liashenko, A.; Piskorz, P.; Komaromi, I.; Martin, R. L.; Fox, D. J.; Keith, T.; Al-Laham, M. A.; Peng, C. Y.; Nanayakkara, A.; Challacombe, M.; Gill, P. M. W.; Johnson, B.; Chen, W.; Wong, M. W.; Gonzalez, C.; Pople, J. A. *Gaussian 09*, revision C.02; Gaussian, Inc.: Wallingford, CT, 2004.
(44) Xiao, D.; Fu, L.; Liu, J.; Batista, V. S.; Yan, E. C. Y. *J. Mol. Biol* **2012**, *421*, 537−547.
(45) Castano, S.; Desbat, B.; Dufourcq, J. *Biochim. Biophys. Acta, Biomembr.* **2000**, *1463*, 65−80.
(46) Buffeteau, T.; Le Calvez, E.; Castano, S.; Desbat, B.; Blaudez, D.; Dufourcq, J. *J. Phys. Chem. B* **2000**, *104*, 4537−4544.
(47) Tamm, L. K.; Tatulian, S. A. *Q. Rev. Biophys.* **1997**, *30*, 365−429.
(48) Barth, A.; Zscherp, C. *Q. Rev. Biophys.* **2002**, *35*, 369−430.
(49) Rozenberg, M.; Shoham, G. *Biophys. Chem.* **2007**, *125*, 166−171.
(50) Lal, B. B.; Nafie, L. A. *Biopolymers* **1982**, *21*, 2161−2183.
(51) Krimm, S.; Dwivedi, A. M. *J. Raman Spectrosc.* **1982**, *12*, 133−137.
(52) Dwivedi, A. M.; Krimm, S. *Biopolymers* **1982**, *21*, 2377−2397.
(53) Kubelka, J.; Keiderling, T. A. *J. Phys. Chem. A* **2001**, *105*, 10922−10928.
(54) Amado, A. M.; Ribeiro-Claro, P. J. A. *J. Chem. Soc., Faraday Trans.* **1997**, *93*, 2387−2390.
(55) Weidner, T.; Breen, N. F.; Drobny, G. P.; Castner, D. G. *J. Phys. Chem. B* **2009**, *113*, 15423−15426.
(56) Zhao, X.; Ong, S.; Wang, H.; Eisenthal, K. B. *Chem. Phys. Lett.* **1993**, *214*, 203−207.
(57) Garand, E.; Kamrath, M. Z.; Jordan, P. A.; Wolk, A. B.; Leavitt, C. M.; McCoy, A. B.; Miller, S. J.; Johnson, M. A. *Science* **2012**, *335*, 694−698.
(58) Nagornova, N. S.; Rizzo, T. R.; Boyarkin, O. V. *Science* **2012**, *336*, 320−323.